Enzyme and Microbial Technology 100 (2017) 20–27

Contents lists available at ScienceDirect

Enzyme and Microbial Technology

journal homepage: www.elsevier.com/locate/emt

Enzymatic biosensor based on entrapment of D-amino acid oxidase on gold nanofilm/MWCNTs nanocomposite modified glassy carbon electrode by sol-gel network: Analytical applications for D-alanine in human serum

Yalda Shoja, Amir Abbas Rafati *, Javad Ghodsi

Department of Physical Chemistry, Faculty of Chemistry, Bu-Ali Sina University, P.O. Box 65174, Hamedan, Iran

ARTICLE INFO

Article history:
Received 18 September 2016
Received in revised form 31 January 2017
Accepted 1 February 2017
Available online 2 February 2017

Keywords:
Biosensor
D-Amino acid oxidase
MWCNT
Au nanostructures
Enzyme immobilization

ABSTRACT

Sensing and determination of D-alanine is studied by using an enzymatic biosensor which was constructed on the basis of D-amino acid oxidase (DAAO) immobilization by sol-gel film onto glassy carbon electrode surface modified with nanocomposite of gold nanofilm (Au-NF) and multiwalled carbon nanotubes (MWCNTs). The Au-NF/MWCNT nanocomposite was prepared by applying the potentiostatic technique for electrodeposition of Au-NF on the MWCNT immobilized on glassy carbon electrode surface. The modified electrode is investigated by scanning electron microscopy (SEM), energy dispersive X-ray spectroscopy (EDX), linear sweep voltammetry (LSV) and cyclic voltammetry(CV) techniques. The linear sweep voltammetry was used for determination of D-alanine and the results showed an excellent linear relationship between biosensor response and D-alanine concentration ranging from 0.25 μM to 4.5 μM with correction coefficient of 0.999 (n = 20). Detection limit for the fabricated sensor was calculated about 20 nM (for S/N = 3) and sensitivity was about 56.1 $\mu A \mu M^{-1} cm^{-2}$. The developed biosensor exhibited rapid and accurate response to D-alanine, a good stability (4 weeks) and an average recovery of 98.9% in human serum samples.

1. Introduction

D-Amino Acids (DAAs) rarely occur naturally in organisms except for some bacteria. It has been reported that the presence of DAAs can verify the bacterial contamination and also can decrease nutritional value of food products [1]. For example, some DAAs have been detected in bacterial cell wall, plants and even vertebrates; thus, the content of these amino acids can be used to measure bacterial contamination [2–4]. Furthermore, amounts of DAAs in the brain are related to several neurological and psychiatric diseases like Alzheimer in which the grey and white matter of Alzheimer brains contain D-aminoacid two to four times higher than the respective region of normal brains [5–7]. Therefore, the sensitive monitoring of DAAs content is necessary in medicine, foodstuff and nutritional science.

Various analytical techniques have been employed for DAAs measurement including capillary electrophoresis [8], gas chromatography [9], spectrophotometry [10] and high-performance liquid chromatography (HPLC) [11]. Besides being sensitive and reliable, these methods are usually very expensive, with low selectivity and long time-consuming sample preparation, too slow to be used in the food industry, need to specialized equipment and require a skilled person to operate [7,12]. Nevertheless, electrochemical techniques are the most powerful methods for electroactive species detection. Among the electrochemical methods, biosensors represent the best performance since they are simple, inexpensive, fast responsive, high sensitive and selective, specific and accurate technique. Thus, biosensors are very suitable instruments for routine analysis in quality control measurements, biomedical, nutritional, clinical and pharmaceutical analysis [13–20].

In D-amino acid biosensor, D-amino acid oxidase (DAAO) is immobilized on different transducers in which DAAO (EC 1.4.3.3, DAAO) is a flavo enzyme that catalyzes the oxidation of D-isomers of amino acids with absolute stereospecificity according to this general reaction:

$$\text{D-Aminoacid} + O_2 + H_2O + \text{DAAO} \rightarrow \alpha\text{-ketoacid} + H_2O_2 + NH_3 \quad (1)$$

* Corresponding author.
E-mail addresses: aa.rafati@basu.ac.ir, rafati.aa@yahoo.com (A.A. Rafati).

http://dx.doi.org/10.1016/j.enzmictec.2017.02.001
0141-0229/

The hydrogen peroxide content produced is determined electrochemically, that is directly proportional to the concentration of DAAs. Some researchers reported biosensors detecting the DAA by measurement of the H_2O_2generated by the DAAO catalyzed reaction [21]. On the other hand DAA biosensors often have some disadvantages such as low conductivity, low reproducibility, high response time, low stability and low sensitivity in biological fluids such as blood. Therefore, development of biosensor is still in need for D-aminoacid measurement in various real samples. Therefore, the traditional electrodes in biosensors can be modified with different materials to obtain the optimal electrochemical properties. In recent years different nanomaterials have been prepared with particular properties for applying in various fields [22,23]. For example, the performance of biosensors can be improved by using nanodimension materials as modifier [24,25]. Regarding this point, gold nanostructures (Au NSs) have attracted great interests due to their excellent electrical conductivity, enhancement of electron transfer rate between electrode and electroactive analytes, good biocompatibility, large surface-to-volume ratios and unique electro catalytically towards analyte molecules such as H_2O_2 [26–29]. Meanwhile, carbon nanotubes have been widely used in biosensor fields because of their large effective surface area, high electric conductivity, excellent biocompatibility, significant mechanical strength and high chemical stability [30]. Large effective surface area has caused carbon nanotubes to become an appropriate platform to load metallic nanostructures. As a new efficient application of carbon nanotubes in biosensors, the carbon nanotube-metal nanocomposites possess the individual properties like synergistic effect with enzymes that can be used in modified biosensors [31,32]. Electrochemical reduction methods were applied for construct carbon nanotube-metal nanocomposite as effective, simple and fast approaches since they do not require the use of chemical materials as protecting agent or reducing agent which can decrease catalytic activity of deposited metal nanostructure [33,34]. Sol-gel was used as a porous network for an effective physical enzyme immobilization because of its appropriate advantages such as large surface areas, high mechanical and thermal stability, great ion exchange capacities, chemically inert, biocompatibility, high permeability, nontoxicity and electro-inactive in aqueous medium [35,36].

In this work, we described the fabrication of noveland improved D-alanine biosensor by immobilized DAAO onto glassy carbon that was modified with the carbon nanotube gold nanofilmnanocomposite (Au-NF/MWCNT). Then, DAAO was immobilized by sol-gel on to Au-NF/MWCNT/GC electrode. At the end, the application of prepared biosensor was investigatedin measurement of D-alanine in human serum.

2. Experimental

2.1. Chemicals

Tetraethyl orthosilicate (TEOS) was obtained from Merck (Germany) and used as received. DAAO (EC 1.4.3.6, DAAO) from porcine kidney (1.5 units mg^{-1} solid), D-alanine, uric acid, folic acid, ascorbic acid and $HAuCl_4$were purchased from Sigma-Aldrich Chemical Co. used without further purification. Multiwalled carbon nanotubes (MWCNTs) were purchased from Neutrino. All the other chemicals used were of analytical reagent grade. Double distilled water was used in all experiments for preparation of solutions. The phosphate buffer solutions were used as supporting electrolytes by dissolving Na_2HPO_4 and NaH_2PO_4 salts in double distilled water and pH values were adjusted with HCl and NaOH solutions.

2.2. Apparatus and procedures

Electrochemical measurements were carried outusing a computer-controlled μ-Auto lab modular electrochemical system (PGSTAT101, the Netherlands), driven with NOVA Software (upgrade 1.10). Scanning electron microscopy (SEM) and energy dispersive X-ray spectroscopy (EDS) were done by VEGA TESCAN SEM. Linear sweep voltammetric and cyclic voltammetric experiments were carried out in a voltammetric cell including three electrode systems of GCE (diameter 3 mm) as working electrode, an Ag/AgCl (saturated potassium chloride) as reference electrode and a platinum foil as counter electrode (all from Azar Electrode Co., Iran).All the electrochemical experiments were performed at room temperature in air pressure.

2.3. Modification of GCE with MWCNTs

The GCE (diameter 3 mm) was first polished with alumina slurry and ultrasonically cleaned from adsorb particles. Then, it was washed with double distilled water and dried with a nitrogen gas stream. 15 mg of multiwalled carbon nanotubes (MWCNTs) were dissolved in 10 mL of acetone and then dispersed in ultrasonic bath for 5 min. Homogeneous black solution was obtained from this process. The MWCNTs coated glassy carbon electrode was prepared by dropping 35 μL of MWCNTs solution on the electrode surface by micro-syringe. Then, the electrode was dried in air to form a MWCNT film on the glassy carbon electrode surface.

2.4. Electrodeposition of gold nanofilm on MWCNT/GCE

For electrodeposition of gold nanofilm (Au-NF) on the MWCNT/GC electrode surface, the potentiostatic technique was employed [31]. The electrodeposition was done in stirring KNO_3 solution (0.1 M) containing 0.2 mM $HAuCl_4$ at a potential of −0.2 V (*vs.* Ag/AgCl sat. KCl) for 60 s. The obtained electrode was thoroughly washed with deionized water and dried in air at room temperature before use. This modified glassy carbon electrode was called Au-NF/MWCNT/GCE.

2.5. Fabrication of the sol-gel/DAAO/Au-NF/MWCNT/GCE

Sol–Gel solution was prepared by mixing 5 mL of TEOS, 1.5 mL of distilled water and 100 μL of 0.1 M HCl at room temperature. A solution of DAAO with concentration of 10 mg/mL was prepared by dissolution appropriate amount of enzyme in sodium phosphate buffer solution (100 mM, pH = 9).

Then, 10 μL of DAAO solution was dropped on Au-NF/MWCNT/GCE to prepare DAAO/Au-NF/MWCNT/GC electrode. Ultimately to physically immobilize DAAO on Au-NF/MWCNT/GCE, 10 μL of sol-gel solution was dropped on DAAO/Au-NF/MWCNT/GCE. Obtained electrode was left for 15 min at room temperature to sol-gel film forming and then washed with sodium phosphate buffer for several times to release the un-immobilized enzymes. Scheme 1 depicts the schematic representation of Sol-Gel/DAAO/Au-NF/MWCNT/GCE fabrication steps. All these steps were performed at room temperature.

3. Results and discussion

3.1. Characterization of modified glassy carbon electrode

The SEM images of MWCNT deposited on GCE and gold nanofilm (Au-NF) electrodeposited on MWCNT/GCE are shown in Fig. 1a and b, respectively. As can be seen in Fig. 1a, the diameter of pure MWCNT is about 47 nm and after gold deposition; the MWCNT diameter increases about 82 nm. Therefore, it can be concluded

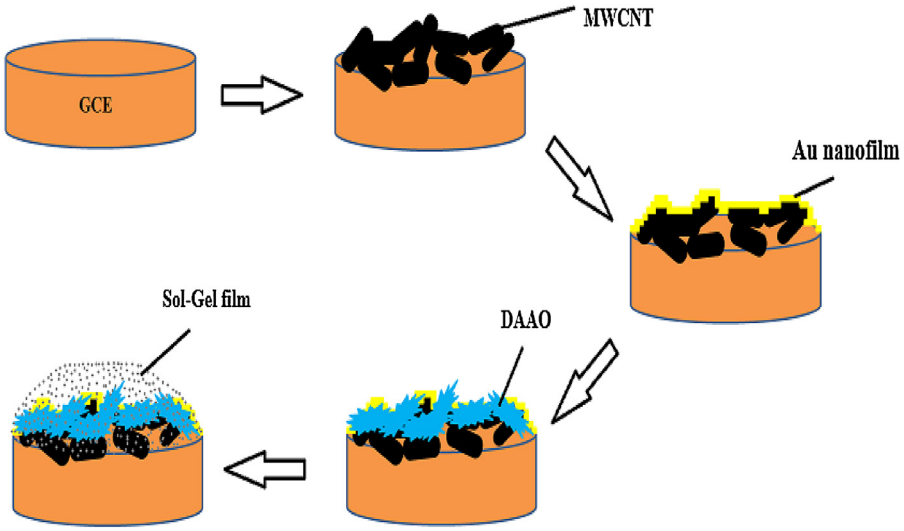

Scheme 1. Fabrication steps of D-alanine biosensor.

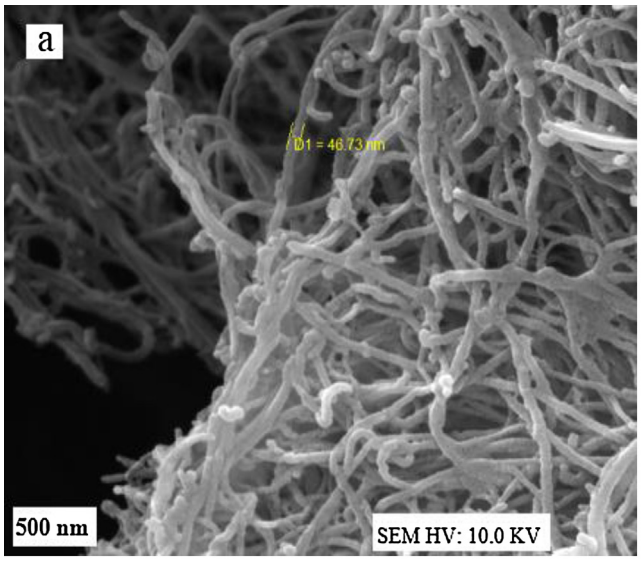

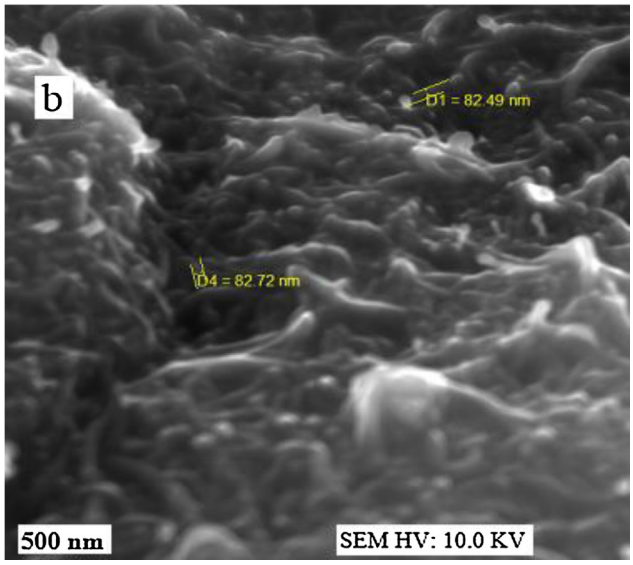

Fig. 1. SEM images of modified GCE (a), MWCNT/GCE and (b) Au-NF/MWCNT/GCE.

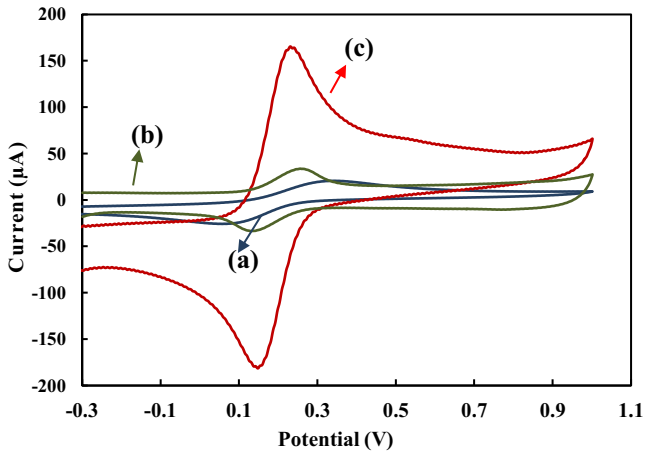

Fig. 2. CV voltammograms obtained with (a) bare GCE, (b) Au-NF/GCE and (c) Au-NF/MWCNT/GCE in 0.1MKCl solution containing 5.0 mM $K_3[Fe(CN)_6]$ at a scan rate of 50 mV/s.

this increasing in diameter is corresponded to electrodeposition of gold nanofilm onto MWCNT/GCE surface with thickness about 35 nm. Based on Fig. S1 (Supporting information), energy dispersive X-Ray analysis (EDX spectrum), confirms the surface of Au-NF/MWCNT/GCE included C and Au elements with 97.6 and 2.4 wt.%, respectively. Therefore, this evidence clearly verifies the existence of Au nanofilm on the MWCNT/GC electrode. Also this low quantity of Au significantly decreases cost of final biosensor.

3.2. Electrochemical behaviours of the Au-NF/MWCNT/GCE

Fig. 2 shows cyclic voltammograms (CVs) of bare GCE (curve a), Au-NF/GCE (curve b) and Au-NF/MWCNT/GCE (curve c) obtained in 0.1 MKCl solution containing 5.0 mM $K_3[Fe(CN)_6]$. The electron transfer rate of electrode is related to peak separation. The smaller peak separation indicates the larger electron transfer rate for electrode.

As can be seen in Fig. 2, the peak separations are about 288.0 mV, 127.0 mV and 83.0 mV for bare GCE, Au-NF/GCE, Au-NF/MWCNT/GCE respectively for the redox processes between $[Fe(CN)_6]^{3-}/[Fe(CN)_6]^{4-}$ couple and these electrodes. Therefore, it can be deduced that this redox process was more reversible on Au-NF/MWCNT/GCE surface than two other electrodes. Another most

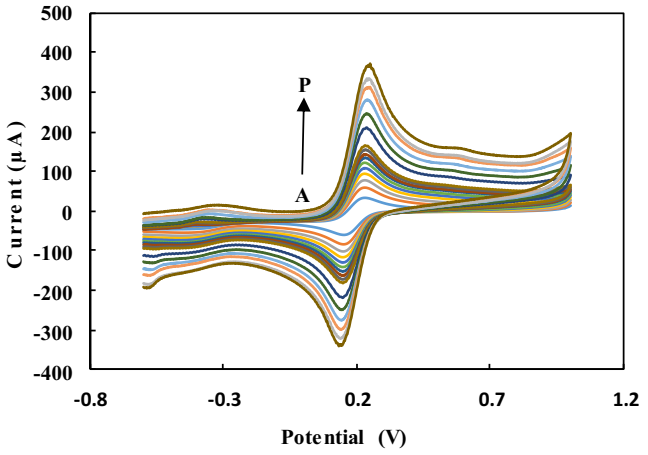

Fig. 3. CV voltammograms of Au-NF/MWCNT/GCE at different scan rates (curves A–P: 10, 20, 30, 40, 50, 60, 70,80, 90, 100, 150, 200, 250, 300, 350 and 400 mV/s), All in 0.1 M KCl solution containing 5.0 mM $K_3[Fe(CN)_6]$.

important parameter for electrode performance is effective surface area that is related to the peak height. To calculate effective surface area of developed biosensor and further electrochemical investigations, we measured the CVs at a series of scan rates ranging from 10 to 400 mV/s in 5.0 mMK_3[Fe (CN)$_6$] solution for bare GCE, Au-NF/GCE and Au-NF/MWCNT/GCE. The results are shown in Fig. 3 and Supporting information section (Figs. S2 and S3).

The peak potentials plotted *vs.* scan rates (Fig. 4). As can be seen from Fig. 4, for Au-NF/MWCNT/GCE peak separation remains almost constant with increasing of scan rate which indicated the high electron transfer rate for this electrode. In contrast to the Au-NF/MWCNT/GCE, for bare GCE, the peak separation increased markedly with increasing of scan rate which implied the limitation due to low electron transfer rate for this electrode.

Furthermore, the Randles–Sevcik equation gives peak current for a reversible process [37]:

$$i_p = (2.69 \times 10^5)n^{3/2}ACD^{1/2}\nu^{1/2} \quad (2)$$

where A is effective surface area (in cm^2), D is the diffusion coefficient (that for $[Fe(CN)_6]^{-4}$ 7.35×10^{-6} cm^2 s^{-1} [38]), n is the number of electrons transferred, ν is the scan rate (in V/s) and C is the bulk concentration (in mol cm^{-3}). According to Eq. (2) anodic peak current is directly proportional with square root of potential scan rate.

Therefore, from the slope of anodic peak current (I_{pa}) *vs.* square root of scan rates (Fig. S4 in Supporting information) for 5.0 mM K_3[Fe (CN)$_6$], $n = 1$ and $D = 7.35 \times 10^{-6}$ cm^2 s^{-1}, effective surface area (A) was calculated about 0.5 cm^2, 1.58 cm^2 and 5.45 cm^2 for bare GCE, Au-NF/GCE and Au-NF/MWCNT/GCE respectively. These results confirmed the effective surface area for Au-NF/MWCNT/GCE is larger than that of two the other electrodes. Consequently, it can be concluded the higher electron transfer rate and larger effective surface area for Au-NF/MWCNT/GCE are related to nanodimension and synergistic effect between Au nanostructure and MWCNT.

3.3. Electrochemical characterization of sol-gel/DAAO/Au-NF/MWCNT/GCE

Fig. 5 shows the CVs of bare GCE (curve a), Sol-Gel/DAAO/GCE (curve b), Sol-Gel/DAAO/Au-NF/GCE (curve c) and Sol-Gel/DAAO/Au-NF/MWCNT/GCE (curve d) in 100 mM PBS (pH = 9), respectively. As can be seen from Fig. 5, CVs of bare GCE and Sol-Gel/DAAO/GCE, (curves a and b), have been matched with each other and they do not show any oxidation and redaction peaks. Therefore, it can be said there is no electron transfer between the DAAO and electrode surface in whole scanning potential range in PBS. Sol-Gel/DAAO/Au-NF/GCE also shows an oxidation peak at nearly 0.86 V and a reduction peak at 0.5 V. These redox peaks are related to the oxidation of deposited Au and reduction of oxidized Au that verify the presence of Au on the GCE surface [37,39]. In CV of Sol-Gel/DAAO/Au-NF/MWCNT/GCE two significant oxidation and reduction peaks were appeared which are potentially the same as Sol-Gel/DAAO/Au-NF/GCE but they are stronger.Itsmay be because of high effective surface area and large surface-to-volume ratio of MWCNTs resulted in more Au with nanofilm structure

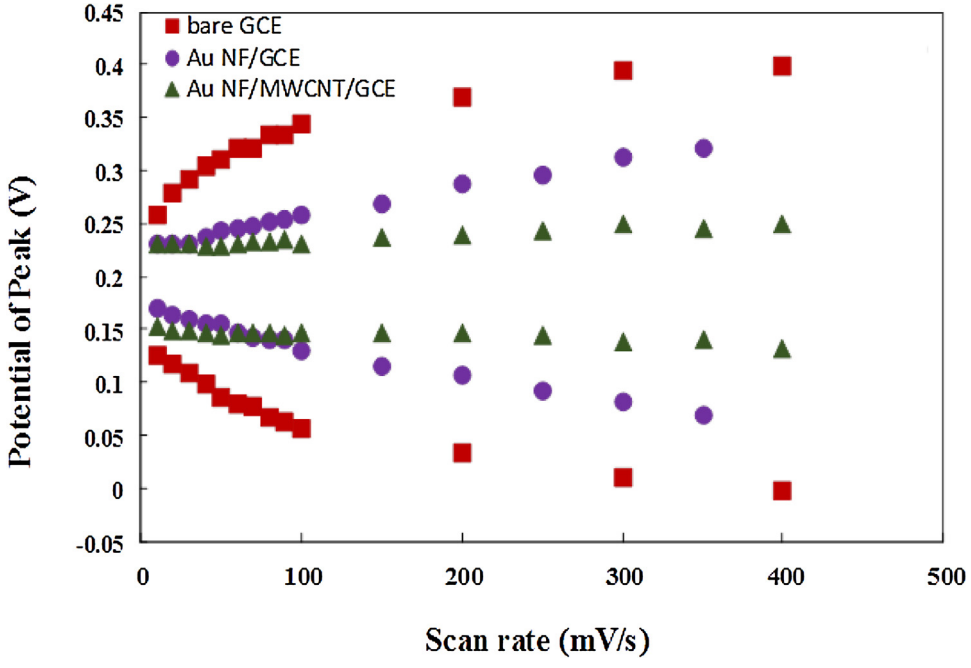

Fig. 4. The cathodic and anodic peak potentials versus the scan rates. All in 0.1 M KCl solution containing 5.0 mM $K_3[Fe(CN)_6]$.

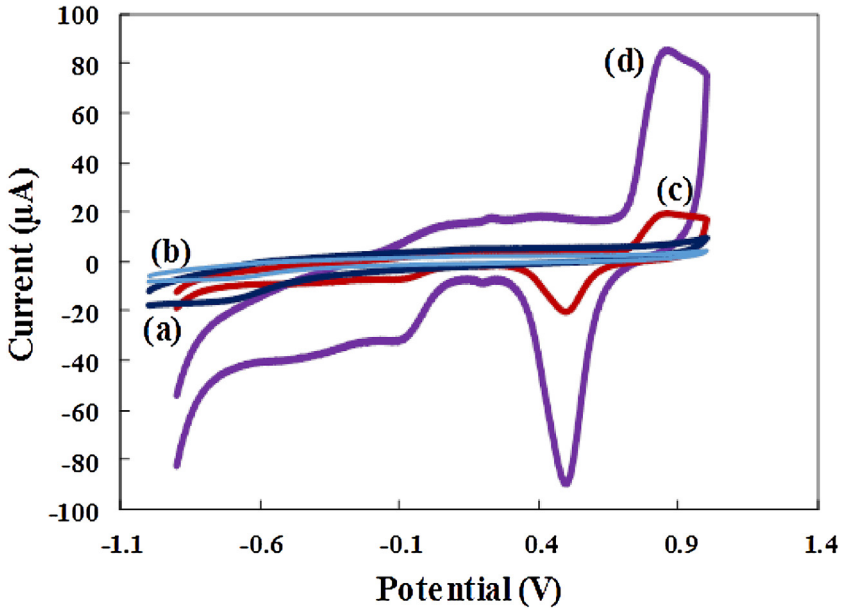

Fig. 5. CV voltammograms of bare/GCE (curve a), Sol-Gel/DAAO/GCE (curve b), Sol-Gel/DAAO/Au-NF/GCE (curve c) and Sol-Gel/DAAO/Au-NF/MWCNT/GCE (curve d) all at scan rate 100 mV/s in PBS (100 mM, pH 9).

deposited on MWCNT/GC electrode surface in compare with bare GC electrode.

It was proved that the maximum current potential of metal oxidation shifted to more negative potentials when macro structure changes to nanostructure that is related to Gibbs free surface energy of the metal particles and their size. In this regard, 'Brainina et al.' showed reducing metal particles size has led to increasing of the Gibbs free surface energy [40,41]. It can be said that Gibbs free surface energy enhancement implies nanostructure activity is higher than bulk structure, which makes lower oxidation potential for nanostructures rather than bulk structures. Fig. S5 (Supporting information) shows LSV voltammograms of Au-NF/GCE (curve a), Au-NF/MWGCE (curve b) and Au-bulk/GCE (curve c) in PBS (pH = 9100 mM). This figure shows the oxidation potential of Au with NF structure was shifted toward less positive value rather than Au-bulk structure which indicates nanostructures has higher Gibbs free surface energy that causes higher electrocatalytic activity. Moreover, MWCNT reduces over voltage, oxidation potential of Au-NF deposited on MWCNTs is lower than Au-NF deposited on bare GCE surface [42]. Therefore, the Au-NF/MWCNT/GCE has the lower oxidation potential than two other electrodes.

3.4. Electrocatalytic response of sol-gel/DAAO/Au-NF/MWCNT nanocomposite film to D-alanine

Fig. 6 shows linear sweep voltammograms (LSVs) of GCE and two different modified GCEs in PBS (100 mM, pH = 9), with D-alanine 4 μM. As can be seen, response of the bare GCE and Sol-Gel/DAAO/GCE toward the reduction of H_2O_2, which was produced from D-alanine oxidation, was obviously negligible (curves a, b). In contrast, Sol-Gel/DAAO/Au-NF/MWCNT/GCE shows remarkable current response toward reduction of H_2O_2 in comparison with bare GCE and Sol-Gel/DAAO/GCE.

The well-defined peaks were observed at −0.66 V and 0.5 V for Sol-Gel/DAAO/Au-NF/MWCNT/GCE, which were due to the reduction of H_2O_2 and Au oxidation respectively (curve c) [29,43]. These results confirm that Au-NF has an excellent electrocatalytic activity for H_2O_2 reduction. In addition, high effective surface area and good conductivity of MWCNT make an enhancement in H_2O_2 reduction peak current because these features increase electrocatalytic active sites for this modified electrode. Therefore, it can be concluded, this significant electrocatalytic activity of Sol-Gel/DAAO/Au-NF/MWCNT/GCE is due to synergistic effect of Au and MWCNT simultaneously present in Au-NF/MWCNT nanocomposite.

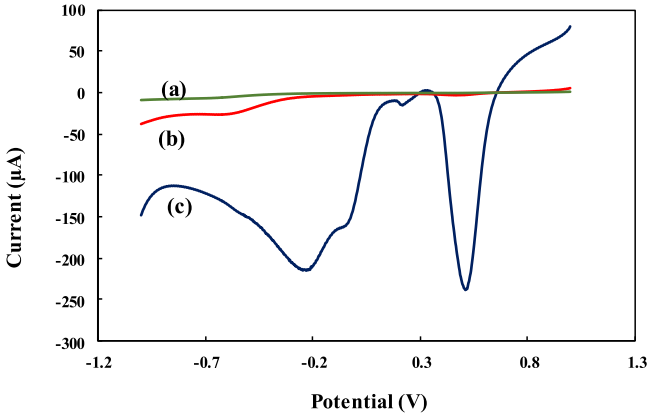

Fig. 6. LSV voltammograms of bare GCE (a) Sol-Gel/DAAO/GCE and (b) Sol-Gel/DAAO/Au-NF/MWCNT/GCE in PBS (100 mM, pH 9) containing 4 μM D-alanine at scan rate 100 mV/s.

3.5. Optimization of DAA biosensor

For optimization of biosensor performance, influence of various parameters such aspH of analyte solution and enzyme concentration were investigated.

3.6. Effect of pH on D-alanine biosensor response

The effect of pH on determination of 4.0 μM D-alanine with Sol-Gel/DAAO/Au-NF/MWCNT/GCE was investigated at different pHs ranging 4–11 in PBS by LSV. The results of this section are shown in Fig. 7. It can be observed that reduction peak potentials of H_2O_2 shift toward more negative values as pH increases. Therefore, it can be suggested H_2O_2 reduction is proton involvement by this biosensor. Furthermore this experiment showed by increasing pH from 4

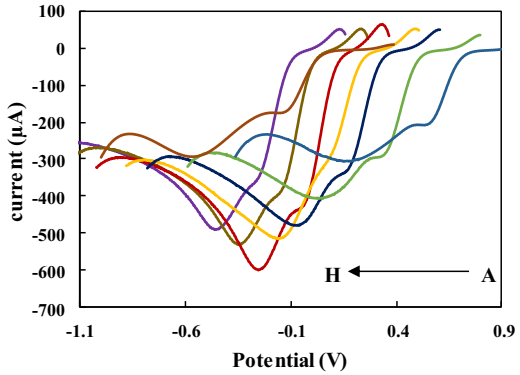

Fig. 7. LSV voltammograms of 4 μM D-alanine in PBS (100 mM) at different pH values: (A) 4, (B) 5, (C) 6, (D) 7, (E) 8, (F) 9, (G) 10 and (H) 11 at scan rate 100 mV/s.

to 9, the peak height increases and then decreases slowly which indicated the enzyme began denaturation (Fig. S6 in Supporting information). Thus the highest peak current occurred at pH 9 for D-alanine, which was chosen as optimized pH for next experiments. Basically,pH influence on this enzymatic biosensor performance is primarily dependent on various parameters such as optimum pH for enzyme activity and zero electric point of substrate and enzyme. It was also reported the pH = 9 is optimized pH for D-amino acid determination in a previous work [44].

3.7. Optimization of DAAO concentration on the biosensor response

Determination of a fixed concentration of D-alanine was done by developed biosensor in various DAAO concentration ranges from 2 mg/mL to 60 mg/mL, for investigation of DAAO concentration influence on biosensor performance. The results of this section showed cathodic current peaks of H_2O_2 increased with increasing of DAAO concentration from 2 mg/mLto 10 mg/mL and then went down as the DAAO concentration went up further above 10 mg/mL.

It can be saidfor the modified electrodes with higher enzyme amounts, a high diffusion barrier may cause a reduced current response or it can decrease electronic communication at the electrode surface [45]. Fig. S7 in Supporting information shows LSV voltammograms of different biosensors modified by various DAAO concentrations and Fig. S8 in Supporting informationshows the optimum concentration of immobilized DAAO (10 mg/mL), which produced the highest reduction current for a fixed amount of D-alanine.

3.8. Calibration curve for determination of D-alanine

Fig. 8a shows the LSV voltammograms of D-alanine obtained by modified biosensor by changing the concentration of D-alanine. It was observed that the H_2O_2 reduction current peaks gradually increase with the increasing of D-alanine concentration.Fig. 9b shows the D-alanine calibration curve obtained by this biosensor under optimal experimental conditions that showed an excellent linear response in the range of 0.25 μM to 4.5 μM with a correlation coefficient of 0.999 (for n = 20). The response time for the biosensor, reaching 90% of its maximum response, was obtained about 10 s.

According to the results of this section, detection limit of modified biosensor was calculated about 20 nM(signal-to-noise ratio S/N = 3) and its sensitivity was found to be

56.1 $\mu A \mu M^{-1}\,cm^{-2}$ (LSV voltammogram in plain and LSV voltammogram with D-alanine concentration close to LOD are shown in Fig. S9 in supporting information).

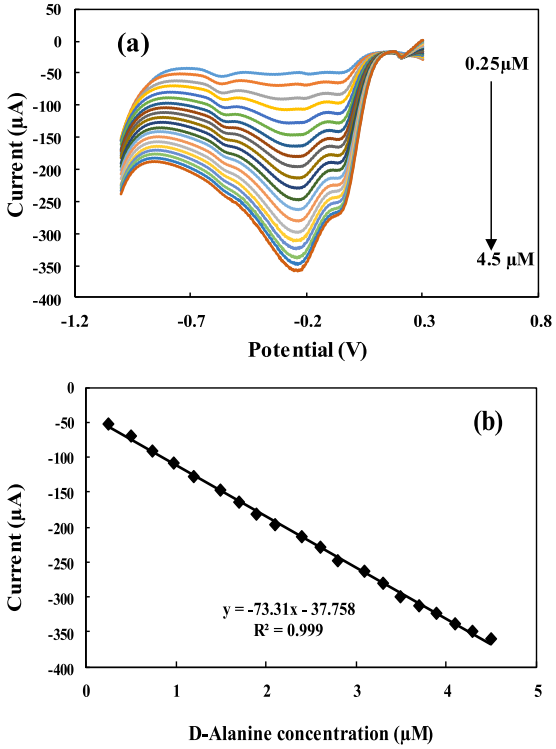

Fig. 8. (a) LSV voltammograms of Sol-Gel/DAAO/Au-NF/MWCNT/GCE in PBS (100 mM, pH 9) upon increasing the concentration of D-alanine; (b) calibration curve obtained from LSV voltammograms data for D-alanine in range 0.25–4.5 μM.

Also, the performance of this modified biosensor is compared with previously reported modified biosensors for D-amino acid determination (Table 1). Furthermore, comparison between the developed biosensor and a simple assay for D-alanine determination, like spectrophotometry, does not show better performances for optical system than the our developed amperometric biosensor due to its detection limit (more than about 0.15 mM) and its narrow concentration range (0.2–1 mM), [1].

For kinetic investigation of the substrate–enzyme, the apparent Michaelis–Menten constant (K_m), is typically used to assess the biological activity of an immobilized enzyme [46]. Smaller Michaelis–Mentenconstant, resulted the high activity of enzyme. K_m can be determined from this basic Michaelis–Menten equation:

$$\frac{1}{\upsilon} = \frac{1}{\upsilon_{max}}\left(\frac{K_m}{[S]} + 1\right) \quad (3)$$

In electrochemical methods, the Lineweaver–Burk equation is:

$$\frac{1}{I} = \frac{1}{I_{max}}\left(\frac{K_m}{[S]} + 1\right) \quad (4)$$

Where peak current (I) is a criterion for reaction rate in this equation, K_m is Michaelis–Menten constant and [S] is substrate concentration respectively [47]. Fig. S10(in supporting information) displays Lineweaver-Burk plot of the Sol-Gel/DAAO/Au-NF/MWCNT/GC electrode at different D-alanine concentration obtained from calibration curve. K_m can be evaluated from slope and intercept of this reciprocal plot. The analysis results showed the K_m and I_{max} values for developedbiosensor were about 4 μM and 588.24 μA, respectively. As can be seen, this value for K_m is much less than that previously reported in other works such as Graphite-Teflon electrode (K_m = 0.25 mM) [44],that confirms the modified biosensor possesses high biological sensitivity toward D-alanine.

Table 1
Comparison between of our developed electrode performance for determination of D-alanine with some methods previously reported.

Support of immobilization	Immobilization methods	Detection limit	Linear range	Working optimum pH	Storage stability	Ref.
Silica gel	Cross-linkage	0.45 μM	1.11–210 μM	5.3	Not Define	[47]
NiHCNFe/PPY/GCE	Cross-linkage	1.5 μM	20–500 μM	7.0	2 months	[7]
Egg shell membrane	Cross-linkage	30 μM	0.05–1.5 mM	7.0	2 months	[48]
Amberzymeoxirane	Cross-linkage	50 μM	0.25–5.0 mM	8.0	2 weeks	[12]
Prussian blue and Nafion layer	Adsorption	1 μM	50–200 μM	7.4	10 days	[49]
Graphite–Teflon Electrode	Not Define	23 μM	5.0–500 μM	9.0	Not Define	[44]
Au-NF/MWCNT/GCE	Sol-Gel	20 nM	0.25–4.5 μM	9.0	4 weeks	This work

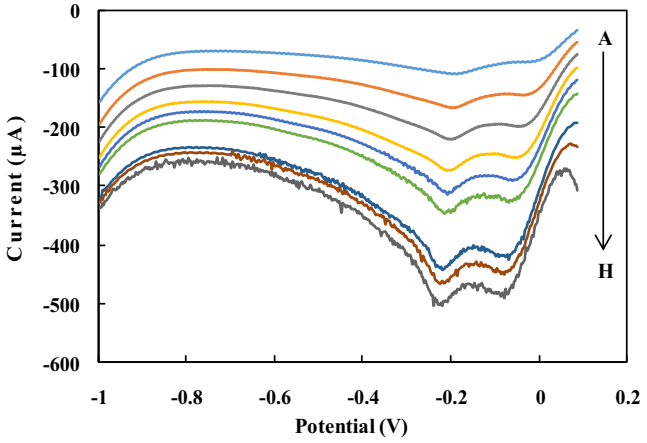

Fig. 9. LSV voltammograms of Sol-Gel/DAAO/Au-NF/MWCNT/GCE in PBS (100 mM, pH = 9.0) containing 5 μM D-alanine at different scan rates (curves A–H: 10, 20, 30, 40, 50, 60, 80, 90 and 100 mV/s).

3.9. Effect of potential scan rate on D-alanine voltammograms

Fig. 9 shows the LSV voltammograms of PBS solution (pH9) containing constant amount of D-alanine (5 μM) at different potential scan rates from 100 mV/s to 1000 mV/s (100, 200,300, 400, 500, 600, 800, 900 and 1000 mV/s) and Fig. S11 (in supporting information) shows the reduction peak current increases with increasing of square root ofthe potentialscan rates in linear relationship in range of 100–1000 mV/s. Therefore, it means that the electrochemical oxidation of D-alanine on Sol-Gel/DAAO/Au-NF/MWCNT/GC electrode is a diffusion controlled process.

3.10. Interference study

In order to evaluate interference effect on the response of D-alanine biosensor, some common interference species (uric, folic, ascorbic acid and L and D-alanine racemic mixed) were investigated by the LSV technique under optimum conditions. The response of D-alanine biosensor in PBS solution (pH = 9)containing 4 μM D-alanine, 8 μM L, D-alanine racemic mixedand 0.01 mM of each other interference species wereconsidered for this study. The results (Fig. S12 in supporting information) showed the influence of uric, folic and ascorbic acid on the D-alanine response is very negligibleand the effect of L and D-alanine racemic mixedon D-alanine biosensor response is similar to pure D-alanine response. It means that this biosensor is only high selectivetoward D-alanine.

3.11. Determination of D-alanine in human serum

The developedbiosensor was successfully applied for measurement of D-alanine in human serum sample. The standard addition technique was used for quantitative analysis of D-alanine after the serum samples were diluted with phosphate buffer solution (pH = 9). The results showed average recovery of D-alanine which was exogenously added in serum samples was about 98.9% (Table 2). It can be said that, according to these results, this biosensor provides a reliable method for the determination of D-amino Acids in biological samples.

Table 2
Results of the recovery analysis of D-alanine spiked in human serum samples.

Spiked (μM)	Found (μM)	Recovery%
–	2.14	–
5	7.2	101.2
10	11.9	97.6
15	17.07	99.5
20	21.6	97.3

3.12. Stability and repeatability of biosensor

Developed biosensor was suitably stable for about 4 weeks. Biosensor retains 85% of initial current response (on the first day of fabrication) after 4 weeks (Fig. S13 in supporting information). Also, it has approximately a same response after 15 successive determinations of a fixed D-alanine solution that shows the fabricated biosensor has a good repeatability(Fig. S14 in supporting information). The biosensor was stored at 4 °C in a refrigerator in sodium phosphate buffer solution in during of stability tests (pH = 9, 100 mM).

4. Conclusion

In summary, the improvedamperometricbiosensor for D-alanine was founded on the basis of physically immobilization of DAAO on glassy carbon electrode modified with Au-NF/MWCNT nanocomposite, by sol-gel to construct a new Sol-Gel/DAAO/Au-NF/MWCNT modified GC electrode.The developed biosensor showed accurate, high selectivity and sensitivity response to D-alanine detection. Furthermore, this biosensor has excellent linear response in wide concentration range (0.25–4.5 μM), low detection limit (20 nM), an average recovery of about 98.9% in real samples, good reproducibility and good storage stability (4weeks). These results confirmed an efficient catalytic property of GC electrode modified with Sol-Gel/DAAO/Au-NF/MWCNT nanocomposite for detection and determination of D-alanine that could offer a reliable biosensor for other DAAs.

Acknowledgment

The authors greatly acknowledge Bu-Ali Sina University for the financial support from the Grant Research Council.

Appendix A. Supplementary data

Supplementary data associated with this article can be found, in the online version, at http://dx.doi.org/10.1016/j.enzmictec.2017.02.001.

References

[1] B. Batra, S. Kumari, C.S. Pundir, Construction of glutamate biosensor based on covalent immobilization of glutmate oxidase on polypyrrole nanoparticles/polyaniline modified gold electrode, Enzyme Microb. Technol. 57 (2014) 69–77.
[2] E. Rosini, G. Molla, C. Rossetti, M.S. Pilone, L. Pollegioni, S. Sacchi, A biosensor for all D-amino acids using evolved D-amino acid oxidase, J. Biotechnol. 135 (2008) 377–384.
[3] S. Sacchi, E. Rosini, L. Caldinelli, L. Pollegioni, Biosensors for D-amino acid detection, Mol. Biol. 794 (2012) 313–324.
[4] I. Gandolfi, G. Palla, L. Delprato, F.D. Nisco, R. Marchelli, C. Salvatori, D-amino acids in milk as related to heat treatments and bacterial activity, J. Food Sci. 57 (1992) 377–379.
[5] M.F. Mora, C.E. Giacomelli, C.D. Garcia, Interaction of D-amino acid oxidase with carbon nanotubes: implications in the design of biosensors, Anal. Chem. 81 (2009) 1016–1022.
[6] B.X. Li, Z.J. Zhang, Chemiluminescence flow biosensor for determination of total D-amino acid in serum with immobilized reagents, Sens. Actuators B 69 (2000) 70–74.
[7] S. Lata, C.S. Pundir, Fabrication of an amperometric d-amino acid biosensor based on nickel hexacyanoferratepolypyrrole hybrid film deposited on glassy carbon electrode, Bioprocess Biosyst. Eng. 36 (2013) 81–89.
[8] Y. Huang, M. Shi, S. Zhao, Quantification of D-Asp and D-Glu in rat brain and human cerebrospinal fluid by microchip electrophoresis, J. Sep. Sci. 32 (2009) 3001–3006.
[9] R. Patzold, H. Bruckner, Gas chromatographic determination and mechanism of formation of D-amino acids occurring in fermented and roasted cocoa beans cocoa powder, chocolate and cocoa shell, Amino Acids 31 (2006) 63–72.
[10] P. Sarkar, I.E. Tothill, S.J. Setford, A.P.F. Turner, Screen-printed amperometric biosensors for the rapid measurement of L-and D-amino acids, Analyst 124 (1999) 865–870.
[11] M. Calabrese, B. Stancher, P. Riccobon, High-performance liquid chromatography determination of proline isomers in Italian wines, J. Sci. Food Agric. 69 (1995) 361–366.
[12] M. Friedman, Chemistry, nutrition, and microbiology of D-amino acids, J. Agric. Food Chem. 47 (1999) 3457–3479.
[13] F.C. Vicentini, L.L.C. Garcia, L.C.S. Figueiredo-Filho, B.C. Janegitz, O. Fatibello-Filho, A biosensor based on gold nanoparticles dihexadecylphosphate, and tyrosinase for the determination of catechol in natural water, Enzyme Microb. Technol. 84 (2016) 17–23.
[14] B. Krajewska, Application of chitin- and chitosan-based materials for enzyme immobilizations: a review, Enzyme Microb. Technol. 35 (2004) 126–139.
[15] A. Afraz, A.A. Rafati, A. Hajian, M. Khoshnood, Electrodeposition of Pt nanoparticles on new porous graphitic carbon nanostructures prepared from biomass for fuel cell and methanol sensing applications, Electrocatalysis 6 (2015) 220–228.
[16] J. Ghodsi, A.A. Rafati, Y. Shoja, M. Najafi, Determination of dopamine in the presence of uric acid and folic acid by carbon paste electrode modified with CuO nanoparticles/hemoglobin and multi-walled carbon nanotube, J. Electrochem. Soc. 162 (2015) B69–B74.
[17] J. Ghodsi, A.A. Rafati, Y. Shoja, First report on electrocatalytic oxidation of oxytetracycline by horse radish peroxidase: application in developing a biosensor to oxytetracycline determination, Sens. Actuators B 224 (2016) 692–699.
[18] J. Ghodsi, A.A. Rafati, Y. Shoja, First report on hemoglobin electrostatic immobilization on WO_3 nanoparticles: application in the simultaneous determination of levodopa, uric acid, and folic acid, Anal. Bioanal. Chem. 408 (2016) 3899–3909.
[19] Y. Shoja, A.A. Rafati, J. Ghodsi, Electropolymerization of Ni–LD metallopolymers on gold nanoparticles enriched multi-walled carbon nanotubes as nano-structure electrocatalyst for efficient voltammetric sertraline detection in human serum, Electrochim. Acta 203 (2016) 281–291.
[20] Y. Shoja, A.A. Rafati, J. Ghodsi, Glassy carbon electrode modified with horse radish peroxidase/organic nucleophilic-functionalized carbon nanotube composite for enhanced electrocatalytic oxidation and efficient voltammetric sensing of levodopa, Mater. Sci. Eng. C 58 (2016) 835–845.
[21] I. Taurino, R. Reiss, M. Richter, M. Fairhead, L. Thöny-Meyer, G. De Micheli, S. Carrara, Comparative study of three lactate oxidases from Aerococcusviridans for biosensing applications, Electrochim. Acta 93 (2013) 72–79.
[22] A.A. Rafati, A.A. Borujeni, M. Najafi, A. Bagheri, Ultrasonic/surfactant assisted of CdS nano hollow sphere synthesis and characterization, Mater. Charact. 62 (2011) 94–98.
[23] A.A. Rafati, A.A. Borujeni, M. Najafi, A. Hajian, Synthesis and characterization of supported silica nano hollow spheres with CdS quantum dots, J. Mol. Liq. 174 (2012) 124–128.
[24] C.Y. Liu, J.M. Hu, Hydrogen peroxide biosensor based on the direct electrochemistry of myoglobin immobilized on silver nanoparticles doped carbon nanotubes film, Biosens. Bioelectron. 24 (2009) 2149–2154.
[25] C. Altinkaynak, S. Tavlasoglu, N. Özdemir, I. Ocsoy, A new generation approach in enzyme immobilization: organic-inorganic hybrid nanoflowers with enhanced catalytic activity and stability, Enzyme Microb. Technol. 93-94 (2016) 105–112.
[26] F. Afzali, M.H. Arbab Zavar, G. Rounaghi, N. Ashraf, Gold digital versatile disc platform modified with nano-porous mercury/gold amalgam as a solid-state disposable electrochemical sensor for detection of *para*-nitrophenol, Electrochim. Acta 209 (2016) 654–660.
[27] M. Bao, X. Ma, Sensitive DNA hybridization detection based on the deposition of gold nanoparticle on lyophobic surface, Mater. Sci. Eng. C 32 (2012) 1808–1812.
[28] G. Hu, Y. Ma, Y. Guo, S. Shao, Electrocatalytic oxidation and simultaneous determination of uric acid and ascorbic acid on the gold nanoparticles-modified glassy carbon electrode, Electrochim. Acta 53 (2008) 6610–6615.
[29] A. Afraz, A.A. Rafati, Analytical sensing of hydrogen peroxide on Ag nanoparticles–multiwalled carbon nanotube-modified glassy carbon electrode, J. Solid State Electrochem. 17 (2013) 2017–2025.
[30] N. Hui, F. Chai, P. Lin, Z. Song, X. Sun, Y. Li, S. Niu, X. Luo, Electrodeposited conducting polyaniline nanowire arrays aligned on carbon nanotubes network for high performance supercapacitors and sensors, Electrochim. Acta 199 (2016) 234–241.
[31] A.A. Rafati, A. Afraz, Amperometric sensing of anti-HIV drug zidovudine on Ag nanofilm-multiwalled carbon nanotubes modified glassy carbon electrode, Mater. Sci. Eng. C39 (2014) 105–112.
[32] X. Wu, Y. Chai, R. Yuan, X. Zhong, J. Zhan, Synthesis of multiwall carbon nanotubes-graphene oxide-thionine-Au nanocomposites for electrochemiluminescence detection of cholesterol, Electrochim. Acta 129 (2014) 441–449.
[33] M.C. Tsai, T.K. Yeh, C.H. Tsai, An improved electrodeposition technique for preparing platinum and platinum–ruthenium nanoparticles on carbon nanotubes directly grown on carbon cloth for methanol oxidation, Electrochem. Commun. 8 (2006) 1445–1452.
[34] L.M. Plyasova, I.Y. Molina, A.N. Gavrilov, S.V. Cherepanova, O.V. Cherstiouk, N.A. Rudina, E.R. Savinova, G.A. Tsirlina, Electrodeposited platinum revisited: tuning nanostructure via the deposition potential, Electrochim. Acta 51 (2006) 4477–4488.
[35] S.S. Rosatto, L.T. Kubota, G.O. Neto, Biosensor for phenol based on the direct electron transfer blocking of peroxidase immobilising on silica–titanium, Anal. Chim. Acta 390 (1999) 65–72.
[36] K. Reddaiah, T.M. Reddy, Electrochemical biosensor based on silica sol–gel entrapment of horseradish peroxidase onto the carbon paste electrode toward the determination of 2-aminophenol in non-aqueous solvents: a voltammetric study, J. Mol. Liq. 196 (2014) 77–85.
[37] J. Wang, Analytical Electrochemistry, 3rd ed., Wiley-VCH, New York, 2006.
[38] W.M. Haynes, Handbook of Chemistry and Physics, 95th ed., CRC Press, 2014.
[39] H. Gomez, H. Lizama, C. Suarez, A. Valenzuea, Effect of thiourea concentration on the electrochemical behavior of gold and copper electrodes in presence and absence of Cu (II) ions, J. Chil. Chem. Soc. 54 (2009) 439–444.
[40] K.Z. Brainina, L. Galperin, E. Vikulova, N.Y. Stozhko, A.M. Murzakaev, O.R. Timoshenkova, Y. Kotov, Gold nanoparticles electrooxidation: comparison of theory and experiment, J. Solid State Electrochem. 15 (2011) 1049–1056.
[41] K.Z. Brainina, L. Galperin, T.Y. Kiryuhina, A.L. Galperin, N.Y. Stozhko, A.M. Murzakaev, O.R. Timoshenkova, Silver nanoparticles electrooxidation: theory and experiment, J. Solid State Electrochem. 16 (2012) 2365–2372.
[42] W.C. Poh, K.P. Loh, W.D. Zhang, S. Triparthy, J.S. Ye, F.S. Shen, Biosensing properties of diamond and carbon nanotubes, Langmuir 20 (2004) 5484–5492.
[43] A. Manivel, S.J. Anandan, Silver nanoparticles embedded phosphomolybdate–polyaniline hybrid electrode for electrocatalytic reduction of H_2O_2, J. Solid State Electrochem. 15 (2011) 153–160.
[44] R. Dominguez, B. Serra, A.J. Reviejo, J.M. Pingarron, Chiral analysis of amino acids using electrochemical composite bienzyme biosensors, Anal. Biochem. 298 (2001) 275–282.
[45] A. Morrin, F. Wilbeer, O. Ngamna, S.E. Moulton, A.J. Killard, G.G. Wallace, M.R. Smyth, Novel biosensor fabrication methodology based on processable conducting polyaniline nanoparticles, Electrochem. Commun. 7 (2007) 317–322.
[46] Y. Zou, C. Xiang, L. Sun, F. Xu, Glucose biosensor based on electrodeposition of platinum nanoparticles onto carbon nanotubes and immobilizing enzyme with chitosan-SiO_2 sol–gel, Biosens. Bioelectron. 23 (2008) 1010–1016.
[47] F.R. Shu, G.S. Wilson, Rotating ring-disk electrode for surface catalysis studies, Anal. Chem. 48 (1976) 1679–1686.
[48] G. Zhang, D. Liu, S. Shuang, M.F. Martin, A homocysteine biosensor with eggshell membrane as an enzyme immobilization platform, Sens. Actuators B 114 (2006) 936–942.
[49] M. Wcislo, D. Compagnone, M. Trojanowicz, Enantioselective screen-printed amperometric biosensor for the determination of d-amino acids, Bioelectrochem 71 (2007) 91–98.